

A Video Compression Scheme with Optimal Bit Allocation among Segmentation, Motion and Residual Error

Guido M. Schuster

U.S. Robotics, Network Systems Division
Advanced Technologies Research Center
1800 W. Central Rd.
Mount Prospect, Illinois 60056-2293
Tel: (847) 222-2486
Fax: (847) 222-2266
E-mail: gschuste@usr.com

and

Aggelos K. Katsaggelos
Northwestern University
Department of Electrical and Computer Engineering
McCormick School of Engineering and Applied Science
Evanston, Illinois 60208-3118
Tel: (847) 491-7164
Fax: (847) 491-4455
E-mail: aggk@ece.nwu.edu

Abstract

In this paper we present a theory for the optimal bit allocation among quad-tree (QT) segmentation, displacement vector field (DVF) and displaced frame difference (DFD). The theory is applicable to variable block size motion compensated video coders (VBSMCVC), where the variable block sizes are encoded using the QT structure, the DVF is encoded by first order differential pulse code modulation (DPCM), the DFD is encoded by a block based scheme and an additive distortion measure is employed.

We derive an optimal scanning path for a QT which is based on a Hilbert curve. We consider the case of a lossless VBSMCVC first, for which we develop the optimal bit allocation algorithm using Dynamic Programming (DP). We then consider a lossy VBSMCVC, for which we use Lagrangian relaxation and show how an iterative scheme, which employs the DP-based solution, can be used to find the optimal solution. We finally present a VBSMCVC, which is based on the proposed theory, which employs a DCT based DFD encoding scheme. We compare the proposed coder with H.263. The results show that it outperforms H.263 significantly in the rate distortion sense, as well as in the subjective sense.

EDICS: IP 1.1 Coding

List of Figures

| | | |
|----|---|----|
| 1 | Quad-tree structure: (a)-(c) scanning path of the different levels; (d)Image block with data to be represented and overall scanning path; (e) node indices and leaf ordering; (f) encoded quad-tree | 28 |
| 2 | The four possible first order Hilbert curves (-) with the respective second order Hilbert curves underneath (-). The orientations $O_{l,i}$ are shown on top of the squares and the orientations $O_{l-1,4*i+j}$ are shown in the corners of the smaller squares. | 29 |
| 3 | Recursive Hilbert curve generation: a) first order Hilbert curve of orientation 0, b) second order Hilbert curve, c) third order Hilbert curve | 29 |
| 4 | The multilevel trellis for $N = 5$ and $n_0 = 3$ | 30 |
| 5 | The recursive rule for the generation of the $T_{l,i}$ and $F_{l,i}$ sets | 30 |
| 6 | The recursive distribution of the quad-tree encoding cost among the trellis nodes for a quad-tree of depth 4 and the optimal state sequence | 31 |
| 7 | Quad-tree decomposition corresponding to the optimal state sequence | 31 |
| 8 | Modified Hilbert scan for level $n_0 = 3$ of a QCIF frame. | 32 |
| 9 | Rate and distortion comparison between TMN6 and the optimal coder, where the TMN6 distortion is the target distortion of the optimal coder. | 33 |
| 10 | Left: The optimal encoding mode selection, (i) Inter mode, (s) Skip mode, (p) Prediction mode and (a) Intra mode; Right: the optimal DVF, both are for the 16 th frame of the “Mother and Daughter” sequence. | 33 |
| 11 | Rate and distortion comparison between TMN6 and the optimal coder, where the TMN6 rate is the target rate of the optimal coder. | 34 |
| 12 | Rate and distortion comparison between TMN6 and the optimal coder, where the distortion of the optimal coder is fixed. | 34 |

List of Tables

| | | |
|---|--|----|
| 1 | Average rate distortion comparison for the “Mother and Daughter” sequence between TMN6 and the proposed optimal coder for different modes of operation | 30 |
|---|--|----|

1 Introduction

Video compression attracted considerable attention over the last decade [1, 2, 3]. Several standards for video coding such as MPEG-1 [4], MPEG-2 [5], H.261 [6] and most recently H.263 [7] have been established. There is a large redundancy in any video sequence which has to be exploited by every efficient video coding scheme. This redundancy is divided into temporal and spatial. The temporal redundancy is usually reduced by motion compensated prediction of the current frame from a previously reconstructed frame, whereas the spatial redundancy left in the prediction error is commonly reduced by a transform coder or a vector quantizer. Video coders which use the concept of motion compensated prediction are henceforth called motion compensated video coders (MCVC). All existing video standards belong to this class of video coders. In an MCVC, the original video sequence is represented by the displacement vector field (DVF) and the displaced frame difference (DFD).

One of the drawbacks of most video coders is the fixed block size used for motion estimation and encoding of the DFD. This is the case with the video coding standards with the only exception represented by H.263 [7], the latest video coding standard, which offers the “Advanced Prediction Mode”. This mode contains the option of splitting a 16×16 macro block into four 8×8 blocks. If the macro block is split, then a separate motion vector is transmitted for each of the four 8×8 blocks.

It is well known, that the block size controls the tradeoff between the reliability of the DVF estimate, which increases with the size of the block, and the ability to reduce the energy of the DFD, which decreases with the size of the block [8]. Therefore, a variable block size should be used which adapts to the contents of the scene. Another motivation for the use of a variable block size comes from the object oriented video compression approach [9]. A fixed block size is equivalent to the claim that every object in the scene is made up of equally sized square blocks, which is certainly not the case. An object oriented approach finely segments the scene into objects with different motion. There are two major problems with an object oriented approach: (a) An accurate estimate of the segmentation is required to find the motion information, but on the other hand, one needs the motion information to find the segmentation; (b) The segmentation needs to be encoded and this requires a considerable part of the available bit rate, especially at low bit rates, since the segmentation can be very detailed.

A variable block size coder is a good compromise between the detailed segmentation of the object oriented approach and the coarse and arbitrary segmentation of a fixed block size coding scheme. It can adapt to a scene which is not possible for a fixed block size approach. The bit rate needed for the transmission of the variable block size is much smaller than the bit rate required for the representation of

the segmentation of an object oriented scheme.

The nesting of blocks of different sizes in the image plane requires some underlying structure. For this purpose, most variable block size motion compensated video coders (VBSMCVC) use the quad-tree (QT) data structure to segment the image plane [10, 11, 12]. A fundamental problem of a VBSMCVC is the bit allocation between the QT, DFD and the DVF. In this paper we present a general theory which uses operational rate-distortion curves to solve this problem for a finite set of admissible quantizers and motion vectors.

There have been previous attempts to solve the optimal tradeoff between segmentation, motion and residual error. In [12], a VBSMCVC is presented which uses a mean value QT structure to encode the DFD. The motion estimation is based on block matching and is done for a fixed block size. The optimization of the DVF with respect to the resulting QT is achieved by a local exhaustive search where every motion vector is perturbed by ± 1 pixel and the resulting DFD is encoded using the QT structure. In this scheme, the block size for the motion estimation is kept constant and is not adapted to the scene contents. This leads to an inefficient encoding of the DFD. Also the tradeoff between the QT, the DFD and the DVF is not optimal in the rate distortion sense.

In [13], the tradeoff between the DVF and the DFD is addressed. This is done in the framework of a multi grid block matching scheme. A stochastic model is assumed for the distribution of the DFD and the entropy of a given block is calculated based on observed statistics. This entropy is then used to decide if a block should be split into four smaller blocks with their own motion vectors, or if the block should be kept as a basic unit. In this scheme, the cost for encoding the segmentation is not taken into account. Also the entropy estimation is based on a stochastic model which assumes that the DFD is directly encoded, i.e., no transform coding or vector quantization is applied. Furthermore the DVF is sent using entropy coding of the motion vectors, but because of the high spatial correlation in the DVF, a DPCM based scheme should be used. The biggest drawback is that the resulting distortion is not considered in this scheme and therefore any reduction in the bit rate can easily be offset by an increase in distortion.

In [10], a variable block size motion estimator is presented. It is implied that the motion vectors are encoded by pulse code modulation and hence the resulting optimization procedure is quite simple and in fact equivalent to the one presented in [11]. This scheme has the same shortcoming as the previous one. Since the DVF exhibits a large spatial correlation, an efficient video coding scheme should use a predictive approach for encoding the DVF.

In [14], the optimal bit allocation problem for lossless video coders is studied. The authors use a

stochastic model which has been derived in [13] to find a formula for the entropy of the DFD as a function of the DVF accuracy. The stochastic model derived in [13] cannot be applied if the DFD is encoded by a sophisticated encoding scheme.

The problem addressed in [15, 16] is that of efficient mode selection for block based motion compensated video coders and a Lagrangian multiplier multiplier method and DP based approach is presented. This approach is very similar to the one we proposed in [17] for the same problem in the context of H.263. The Lagrangian multiplier method and DP are also used in the presented work to solve the tradeoff between motion, segmentation and residual error optimally.

Since we use a finite set of admissible quantizers for which the rate distortion points have to be evaluated, the presented theory results in very efficient video coders, but the computational complexity is higher than in a scheme where the rate distortion points are based on a model, such as the one presented in [13]. Nevertheless, the presented scheme has a quadratic time complexity which is very efficient when compared to an exhaustive search.

The paper is organized as follows: In section 2, we define the problem under consideration. In section 3, we introduce an optimal scanning path for a given QT. Then in section 4 we derive the optimal solution for lossless VBSMCVC. This solution is then extended in section 5 to include lossy VBSMCVC. It is common in operational rate distortion theory [18] to only develop the solution to the lossy scheme. By first developing the solution to the lossless scheme, we can clearly show the separation between the Lagrangian multiplier method and the DP approach. In section 6 we develop a lossy video coder as an example of the presented theory and in section 7 we present experimental results with this coder. The paper is summarized in section 8.

2 Notation and assumptions

In this section we introduce the necessary notation and state the assumptions which will be used in the rest of the paper. Our study of the optimal bit allocation between the QT, DVF and DFD is restricted to the frame level. In other words we do not attempt to optimally allocate the bits among the different frames of a video sequence. The reader interested in this problem is referred to [18]. For the rest of this paper we assume that a rate control algorithm has set the maximum number of bits available (R_{max}) or the maximum acceptable distortion (D_{max}) for a given frame.

Let $f_k(\vec{r})$ be the current frame, $\vec{d}_k(\vec{r})$ the DVF and $\tilde{f}_{k-1}(\vec{r})$ the previously reconstructed frame which will be used to predict the current frame. Note that $\tilde{f}_{k-1}(\vec{r})$ does not need to be a frame from the past,

but as in MPEG, this could be a future frame when backward prediction is used. The predicted frame $\hat{f}_k(\vec{r})$ is defined as,

$$\hat{f}_k(\vec{r}) = \tilde{f}_{k-1}(\vec{r} - \vec{d}_k(\vec{r})), \quad (1)$$

and the DFD ($f_k^{DFD}(\vec{r})$) is defined by

$$f_k^{DFD}(\vec{r}) = f_k(\vec{r}) - \hat{f}_k(\vec{r}). \quad (2)$$

In a lossy VBSMCVC, the DFD is quantized and is denoted by

$$f_k^{QDFD}(\vec{r}) = Q[f_k^{DFD}(\vec{r})], \quad (3)$$

where $Q[\cdot]$ is the quantization operator. Finally, the reconstructed frame $\tilde{f}_k(\vec{r})$, is defined by,

$$\tilde{f}_k(\vec{r}) = \hat{f}_k(\vec{r}) + f_k^{QDFD}(\vec{r}). \quad (4)$$

For a lossless VBSMCVC, by definition, $\tilde{f}_k(\vec{r}) = f_k(\vec{r})$.

We assume that the current frame is segmented by a QT. The QT data structure decomposes a $2^N \times 2^N$ image (or block of an image) down to blocks of size $2^{n_0} \times 2^{n_0}$. This decomposition results in an $(N - n_0 + 1)$ -level hierarchy ($0 \leq n_0 \leq N$), where all blocks at level n ($n_0 \leq n \leq N$) have size $2^n \times 2^n$. This structure corresponds to an inverted tree, where each $2^n \times 2^n$ block (called a *tree node*) can either be a *leaf*, i.e., it is not further subdivided, or can branch into four $2^{n-1} \times 2^{n-1}$ blocks, each a *child* node. The tree can be represented by a series of bits that indicate termination by a leaf with a “0” and branching into child nodes with a “1” (see Fig. 1f).

Let $b_{l,i}$ be the block i at level l , and the children of this block are therefore $b_{l-1,4*i+j}$, where $j \in [0, 1, 2, 3]$. The complete tree is denoted by \mathcal{T} and a tree node is identified by the ordered pair (l, i) , where again l is the level and i the number within that level (see Fig. 1e). This ordered pair is called the index of the tree node. Each leaf of \mathcal{T} represents a block which will be used for motion estimation and DFD encoding. For future convenience, let the leafs be numbered from one to the total number of leafs in the QT ($N_{\mathcal{T}}$), from left-to-right and hence in increasing order of the measure $4^{l-n_0} * i$ (this ordering of the leafs is indicated by italic numbers in Fig. 1e).

Let $q_{l,i} \in Q_{l,i}$ be the quantizer for block $b_{l,i}$, where $Q_{l,i}$ is the set of all admissible quantizers for block $b_{l,i}$. Let $m_{l,i} \in M_{l,i}$ be the motion vector for block $b_{l,i}$ where $M_{l,i}$ is the set of all admissible motion vectors for block $b_{l,i}$. Let $s_{l,i} = [l, i, q_{l,i}, m_{l,i}] \in S_{l,i} = \{l\} \times \{i\} \times Q_{l,i} \times M_{l,i}$ be the local state for block $b_{l,i}$, where $S_{l,i}$ is the set of all admissible state values for block $b_{l,i}$. Let $x = [l, i, q, m] \in X = \bigcup_{l=N}^{n_0} \bigcup_{i=0}^{4^{N-l}-1} S_{l,i}$ be

the global state and X the set of all admissible state values. Finally let $x_0, \dots, x_{N_{\mathcal{T}}-1}$ be a global state sequence, which represents the left-to-right ordered leaves of a valid QT \mathcal{T} .

We assume that the frame distortion $D_k(x_0, \dots, x_{N_{\mathcal{T}}-1})$ of the reconstructed frame is the sum of the individual block distortions $d(x_j)$, that is,

$$D_k(x_0, \dots, x_{N_{\mathcal{T}}-1}) = \sum_{j=0}^{N_{\mathcal{T}}-1} d(x_j). \quad (5)$$

Most common distortion measures, such as the mean squared error (MSE), a weighted MSE or the peak signal to noise ratio (PSNR) fall into this class.

We assume that the DVF is encoded by first order DPCM. In other words, the difference between consecutive motion vectors is encoded using entropy coding. In [19], we have developed a theory for the optimal bit allocation between DFD and DVF for motion compensated video coders with fixed segmentation, which also covers higher order DPCM schemes. Because of the variable block sizes, we add the constraint that blocks which belong to the same parent, need to be encoded in sequence. In section (3), we define and derive an optimal scanning path which satisfies the above assumption and constraint.

Based on the first order DPCM assumption, the frame rate $R_k(x_0, \dots, x_{N_{\mathcal{T}}-1})$ can be expressed as follows,

$$R_k(x_0, \dots, x_{N_{\mathcal{T}}-1}) = \sum_{j=0}^{N_{\mathcal{T}}-1} r(x_{j-1}, x_j), \quad (6)$$

where $r(x_{j-1}, x_j)$ is the block rate which depends on the encoding of the current and previous blocks, since the motion vector difference between these two blocks is entropy coded.

3 Optimal scanning path

In this section we address the problem of a “good” scanning path for a given QT. We define and derive an optimal scanning path which is based on a Hilbert curve. By decomposing a $2^N \times 2^N$ image block using a QT into sub-blocks of different sizes ($2^n \times 2^n, n_0 \leq n \leq N$), the problem of a good scanning path arises, since we assume that the DVF is differentially encoded along the scanning path. Note that the variable block sizes are not only used for the DFD but also for the estimation of the DVF. This results in an inhomogeneous motion vector field or, in other words, in a description of the scene where blocks of different sizes move in different directions.

The traditional raster scan (left to right, top to bottom) cannot be applied for variable block sizes since the segmentation of the scene changes from frame to frame. As we have pointed out in section (2), the choices for scanning paths are constrained by the requirement that child blocks which belong to the same

parent block need to be scanned in sequence. Usually, a recursive scanning path is used which traverses the QT in a predefined pattern which is the same for each block. In Fig. 1 an example of a raster scan is shown. Fig. 1a through Fig. 1c show the scanning path at different levels and in Fig. 1d the resulting overall scanning path is displayed. Since the DVF is coded using DPCM along the scanning path, the correlation between successive motion vectors, and therefore the efficiency of the DPCM, strongly depends on the selected scanning path. The following definition explains how we interpret the concept of a “good” scanning path.

Definition 1 *A scanning path is optimal if it connects only neighboring blocks, i.e., blocks which share an edge, and if it visits each block once and only once.*

The motivation behind this definition comes from the observation that an optimal scanning path will lead to highly correlated successive motion vectors, since such vectors will always belong to neighboring blocks. Note that the raster scan path which has been traditionally used in the QT decomposition is suboptimal, as shown in Fig. 1d.

Since the segmentation changes from frame to frame, no fixed scanning path can be employed. On the other hand, no additional information should have to be transmitted to indicate which scanning path was used. Therefore, a good scanning path must be inferable from the transmitted QT and it has to be optimal in the above defined sense.

The optimal scanning path we developed is based on a Hilbert curve. A Hilbert curve has a certain order and the first order Hilbert curve can have one of four orientations, denoted by 0, 1, 2 and 3. Fig. 2 shows the four first order Hilbert curves with the associated second order Hilbert curves drawn beneath it. Note that each second order Hilbert curve consists of four first order Hilbert curves connected by a dotted line and scaled by a factor of $\frac{1}{2}$.

This relationship between first and second order Hilbert curves can be generalized by the following proposed algorithm. This algorithm generates a Hilbert curve of order N and shows the close relationship between a QT and a Hilbert curve. Let $O_{l,i} \in [0, 1, 2, 3]$ be the orientation (scanning order of the blocks $b_{l-1,4*i+j}, j \in [0, 1, 2, 3]$) of block $b_{l,i}$ and let $(\cdot)_4$ denote the modulo 4 operation. The recursion needs to be initialized by the desired orientation of the first order Hilbert curve, say $O_{N,0} = 0$ (upper left figure in Fig. 2). Then we propose to create a Hilbert curve of order N in a Top-Down fashion by calling the function “orient(l, i)” below with the following parameters: orient($N, 0$).

orient(l, i)

$$O_{l-1,4*i+0} = (5 - O_{l,i})4; O_{l-1,4*i+1} = O_{l,i}; O_{l-1,4*i+2} = O_{l,i}; O_{l-1,4*i+3} = 3 - O_{l,i};$$

if $(l - 1 > 1)$

$$\text{orient}(l - 1, 4 * i + 0); \text{orient}(l - 1, 4 * i + 1); \text{orient}(l - 1, 4 * i + 2); \text{orient}(l - 1, 4 * i + 3);$$

The resulting orientations at each QT level l , ($N \geq l \geq 1$) correspond to a Hilbert curve of order $N - l + 1$, hence at level one, the orientations form a Hilbert curve of order N . In Fig. 3 the recursive generation of a third order Hilbert curve is shown. This curve was generated by using the following function call: $\text{orient}(3,0)$. This recursively generated scanning path results in an optimal path, as described by the following Lemma.

Lemma 1 *If the bottom (level n_0) of a fully decomposed QT is scanned by an $(N - n_0)$ -th order Hilbert curve, then the resulting overall scanning path of any QT decomposition is an optimal scanning path.*

Proof: By Induction: Because of the QT based recursive definition of a Hilbert curve, the $(N - n_0)$ -th order Hilbert curve is an optimal scanning path for a completely developed QT, down to level n_0 .

Assume an optimal scanning path and pick any connected sub path visiting four blocks. Since the overall path is optimal, the sub path is optimal too. By merging the four blocks of the sub path into a single block, the neighboring blocks of the four merged blocks are also neighboring blocks of the new single block. Hence the resulting scanning path is optimal. ■

Note that the theory to be developed next does not require that an optimal scanning path is used but only that blocks with a common parent block are scanned in sequence. Nevertheless in all the examples in the rest of the paper, we will use a Hilbert scan. As can be seen from the proof above, every scanning path which is optimal for the fully decomposed QT, is also optimal for every other QT decomposition. Hence one can create other optimal scanning paths. One advantage of the Hilbert scan is that it will result in a highly correlated one-dimensional representation of the image.

4 Lossless VBSMCVC

In this section we study the case of a lossless VBSMCVC. Clearly lossy VBSMCVC are more common but by developing the solution for a lossless VBSMCVC first, we are able to clearly show the separation between the Lagrangian multiplier approach and the DP approach. Since the reconstructed frame is identical to the original frame, the frame distortion is equal to zero and the goal is to minimize the required frame rate for QT, DVF and DFD. This can be stated as follows,

$$\min_{x_0, \dots, x_{N_T-1}} R_k(x_0, \dots, x_{N_T-1}). \quad (7)$$

Since this is a lossless VBSMCVC, the DFD is not quantized, but encoded losslessly. With a slight abuse of notation, let $q_{l,i}$ represent different lossless encoding schemes for block $b_{l,i}$ (i.e., DPCM with different predictor order, etc.), instead of different quantizers. Since we will refer to this algorithm later on, we will still call the $q_{l,i}$'s quantizers in the following derivation.

Since we deal with a finite number of QTs, admissible motion vectors and quantizers, the above optimization problem can be solved by an exhaustive search. The time complexity for such an exhaustive search is extremely high. It can be shown that a lower bound for the number of different QTs is given by $2^{4^{N-n_0}-1}$, where $(N - n_0) \geq 1$. To find a lower bound on the total time complexity we consider the case when the QT is completely decomposed, i.e., the image is segmented into 4^{N-n_0} blocks of size $2^{n_0} \times 2^{n_0}$. We further assume that the cardinality $|S_{n_0,i}|$ of all admissible local states $S_{n_0,i}$ of the leaves is the same. Hence an exhaustive search, using only this single QT requires $|S_{n_0,i}|^{4^{N-n_0}}$ comparisons. Since we have only considered one QT, this is a lower bound on the time complexity for all QTs hence $\Omega_E(|S_{n_0,i}|^{4^{N-n_0}})$, where E stands for exhaustive search. We will show that the upper bound of the proposed algorithm is significantly smaller than this lower bound for an exhaustive search. Note that when we use the term time complexity, we refer to the number of comparisons necessary to find the optimal solution. This does not include the time spent to evaluate the operational rate distortion functions, since this strongly depends on the implementation of a given VBSMCVC.

Note that the dependency in the QT decomposition comes from the fact that the leaves of the QT reflect the block sizes used for motion estimation, and that the difference between two consecutive motion vectors (which do not necessarily belong to blocks of the same size) along the scanning path is encoded by a variable length code. Since the code words for small differences between motion vectors are shorter than for large differences, the optimal solution will lead to an inhomogeneous, but smooth motion field, i.e., a motion field which reflects the real motion quite well. We show next that this dependency between the previous and the current block leads to an optimization problem which can be solved by forward Dynamic Programming (DP) [20], also called the Viterbi algorithm.

4.1 Multilevel trellis

To be able to employ the Viterbi algorithm, a DP recursion formula needs to be established. A graphical equivalent of the DP recursion formula is a trellis where the admissible nodes and the permissible transitions are explicitly indicated. Consider Fig. 4 which represents the multilevel trellis for a 32×32 image block ($N = 5$), with a QT segmentation developed down to level 3 ($n_0 = 3$, block size 8×8). The QT structure is indicated by the white boxes with the rounded corners. These white boxes are not part of the trellis

used for the Viterbi algorithm but indicate the set of admissible state values $S_{l,i}$ for the individual blocks $b_{l,i}$. The black circles inside the white boxes are the nodes of the trellis (i.e., the state values $s_{l,i}$). Note that for simplicity, only two trellis nodes per QT node are indicated, but in general, a QT node can contain any number of trellis nodes. The auxiliary nodes, start and termination (S and T) are used to initialize the DPCM of the motion vectors and to select the path with the smallest cost.

Each of the trellis nodes represents a different way of encoding the block it is associated with. Since the state of a block is defined to contain its motion vector and its quantizer, each of the nodes contains the rate (and distortion, for the lossy VBSMCVC) occurring by predicting the associated block with the given motion vector and encoding the resulting DFD with the given quantizer.

As can be seen in Fig. 4, not every trellis node can be reached from every other trellis node. By restricting the permissible transitions, we are able to force the optimal path to select only valid QT decompositions. Such valid decompositions are based on the fact that at level l , block $b_{l,i}$ can replace four blocks at level $l - 1$, namely $b_{l-1,4*i+0}$, $b_{l-1,4*i+1}$, $b_{l-1,4*i+2}$ and $b_{l-1,4*i+3}$. As we will see later in this section, the QT encoding cost can be distributed recursively over the QT so that each path picks up the right amount of QT segmentation overhead.

Assume that no QT segmentation is used and the block size is fixed at 8×8 . In this case, only the lowest level is used in the trellis in Fig. 4. The transition costs between the trellis nodes would be the rate required to encode the motion vector differences between consecutive blocks along the scanning path. Assume now that the next higher level, level 4, of the QT is included. Clearly the transition cost between the trellis nodes of level 3 stay the same. In addition, there are now transition costs between the trellis nodes of level 4 and also transition cost from trellis nodes of level 3 to trellis nodes of level 4 and vice versa, since each cluster of four blocks at level 3 can be replaced by a single block at level 4. The fact that a path can only leave and enter a certain QT level at particular nodes results in paths which all correspond to valid QT decompositions. Note that every QT node in a path is considered a leaf of the QT which is associated with this path.

In this example, a tree of depth 3 has been used to illustrate how the multilevel trellis is built. For QTs of greater depth, a recursive rule can be derived which leads to the proper connections between the QT levels. Since the Viterbi algorithm is a forward dynamic programming scheme, the optimal solution is found by going through the multilevel trellis from left to right. At any epoch of the Viterbi algorithm, the shortest path is found (see Eq. (18)), over the set of all the admissible nodes of the previous epoch ($F_{n_0,i-1}$), to every node in the set of all admissible nodes at the current epoch ($T_{n_0,i}$).

These two sets, at each epoch, the “from” set $F_{l,i}$ and the “to” set $T_{l,i}$ can be constructed recursively from the sets of the admissible state values $S_{l,i}$ for each block $b_{l,i}$. Consider Fig. 5 which shows a QT node and its four children. Figure 5a, shows the $F_{l,i}$ set which contains all the trellis nodes from which a transition to the right is permissible. Figure 5b, shows the $T_{l,i}$ set which contains all the trellis nodes to which a transition from the left is permissible. Clearly for the top QT level N , $T_{N,0} = S_{N,0}$ and $F_{N,0} = S_{N,0}$, which is the initialization of the recursion. As we will see in section 4.2, only the sets at level n_0 will be used in the Viterbi algorithm (see Eq. (18)) since they define the permissible transitions which in turn enforce the QT structure. These sets can be generated recursively in a Top-Down fashion by calling the function “sets(l, i)” below with the following parameters: sets($N, 0$).

sets(l, i)

$$\begin{aligned}
T_{l-1,4*i+0} &= T_{l,i} \cup S_{l-1,4*i+0}; & F_{l-1,4*i+0} &= S_{l-1,4*i+0}; & T_{l-1,4*i+1} &= S_{l-1,4*i+1}; & F_{l-1,4*i+1} &= S_{l-1,4*i+1}; \\
T_{l-1,4*i+2} &= S_{l-1,4*i+2}; & F_{l-1,4*i+2} &= S_{l-1,4*i+2}; & T_{l-1,4*i+3} &= S_{l-1,4*i+3}; & F_{l-1,4*i+3} &= F_{l,i} \cup S_{l-1,4*i+3}; \\
&& & & & & & \text{if } (l - 1 > n_0) \\
&& & & & & & \text{sets}(l - 1, 4 * i + 0); \text{sets}(l - 1, 4 * i + 1); \text{sets}(l - 1, 4 * i + 2); \text{sets}(l - 1, 4 * i + 3);
\end{aligned}$$

In the presented multi level trellis, the nodes of the respective blocks hold the information about the rate (and in case of a lossy VBSMCVC, the distortion) occurring when the associated block is encoded using the quantizer and motion vector of the node. The rate needed to encode the inhomogeneous motion field is incorporated into the transition cost between the nodes, but so far, the rate needed to encode the QT decomposition has not been addressed.

Since the Viterbi algorithm will be used to find the optimal QT decomposition, each node needs to contain a term which reflects the number of bits needed to split the QT at its level. Clearly, trellis nodes which belong to blocks of smaller size have a higher QT segmentation cost than nodes which belong to bigger blocks.

When the path includes only the top QT level N , then the QT is not split at all, and only one bit is needed to encode this. Therefore the segmentation cost $A_{N,0}$ equals one. For the general case, if a path splits a given block $b_{l,i}$ then a segmentation cost of $A_{l,i} + 4$ bits has to be added to its overall cost function, since by splitting block $b_{l,i}$, 4 bits will be needed to encode whether the four child nodes of block $b_{l,i}$ are split or not. Since the path only visits trellis nodes and not QT nodes, this cost has to be distributed to the trellis nodes of the child nodes of block $b_{l,i}$. How the cost is split among the child nodes is arbitrary since by the recursive definition of the $F_{l,i}$ and $T_{l,i}$ sets, every path which visits a sub-tree rooted by one

child node, also has to visit the other three sub-trees rooted by the other child nodes. Therefore the path will pick up the segmentation cost, no matter how it has been distributed among the child nodes. Since the splitting of a node at level $n_0 + 1$ leads to four child nodes at level n_0 , which can not be split further, no segmentation cost needs to be distributed among its child nodes. In other words, since it is known that the n_0 level blocks cannot be split, no information needs to be transmitted for this event.

These segmentation costs can be generated recursively in a Top-Down fashion by calling the function “seg(l, i)” below with the following parameters: seg($N, 0$). The recursion needs to be initialized with $A_{N,0} = 1$.

seg(l, i)

$$A_{l-1,4*i+0} = A_{l,i} + 4; A_{l-1,4*i+1} = 0; A_{l-1,4*i+2} = 0; A_{l-1,4*i+3} = 0;$$

if ($l - 1 > n_0$)

$$\text{seg}(l - 1, 4 * i + 0); \text{seg}(l - 1, 4 * i + 1); \text{seg}(l - 1, 4 * i + 2); \text{seg}(l - 1, 4 * i + 3);$$

Note that in the above function, the segmentation cost is distributed along the leftmost child. As mentioned before, any other assignment of the segmentation cost will lead to the same result. See Fig. 6 for an illustration of the recursion involved in the assignment of the encoding cost.

Having established the multi level trellis, the forward DP algorithm can be used to find the optimal state sequence $x_0^*, \dots, x_{N_T-1}^*$ which will solve the problem of minimizing the frame rate as expressed in (7).

4.2 Dynamic programming recursion formula

In the previous Section, the multilevel trellis has been established which is a graphical equivalent of the DP recursion formula which is derived in this Section. Again, each node x_j of the multi level trellis contains $R^{QDFD}(x_j)$, the rate needed to encode the quantized DFD of the corresponding block $b_{l,i}$ using the motion vector $m_{l,i}$ and the quantizer $q_{l,i}$, which together with the level l and block number i define the node. In the case of a lossy VBSMCVC, it also contains $D(x_j)$, which is the distortion occurring when the corresponding block is encoded using the given motion vector and quantizer. As shown in the previous section, each node also contains $R^{SEG}(x_j) = A_{l,i}$, which is the recursively distributed QT encoding cost. In addition to that, the transition cost $R^{DVF}(x_{j-1}, x_j)$ is the number of bits required for the encoding of the motion vector difference between node x_{j-1} and node x_j , where $x_{j-1} \in F_{n_0, j-1}$ and $x_j \in T_{n_0, j}$. The dependency between the blocks is expressed by this term and it is the reason for using dynamic programming to solve the optimization problem. Note that $r(x_{j-1}, x_j)$ in Eq. (6) equals $R^{SEG}(x_j) + R^{QDFD}(x_j) + R^{DVF}(x_{j-1}, x_j)$.

As we pointed out earlier, we will also use the algorithm presented in this section to solve the lossy VBSMCVC case. Therefore let us introduce the generic functions $g(x_{j-1}, x_j)$ and $G(x_0, \dots, x_{N_{\mathcal{T}}-1})$ which will be used to derive the DP recursion formula. For the lossless VBSMCVC, this generic functions are defined as follows,

$$g(x_{j-1}, x_j) = R^{SEG}(x_j) + R^{QDFD}(x_j) + R^{DVF}(x_{j-1}, x_j), \quad (8)$$

and

$$G(x_0, \dots, x_{N_{\mathcal{T}}-1}) = \sum_{j=0}^{N_{\mathcal{T}}-1} g(x_{j-1}, x_j). \quad (9)$$

The above discussion and these definitions imply that the following problem is identical to the minimization problem described by Eq. (7).

$$\min_{x_0, \dots, x_{N_{\mathcal{T}}-1}} G(x_0, \dots, x_{N_{\mathcal{T}}-1}). \quad (10)$$

The goal of the DP is to find the optimal state sequence $x_0^*, \dots, x_{N_{\mathcal{T}}-1}^*$ which will minimize Eq. (10). Let $g_k^*(x_k)$ be the minimum cost up to epoch k , where the epochs count the blocks $b_{n_0, k}$, hence $4^{N-n_0} - 1 \geq k \geq 0$,

$$g_k^*(x_k) = \min_{x_0, \dots, x_{k-1}} \sum_{j=0}^k g(x_{j-1}, x_j), \quad (11)$$

where $x_{-1} = S$, the auxiliary starting node. The motivation behind this definition is the fact that $g_{4^{N-n_0}}^*(T)$ is the minimum cost required to traverse the trellis from (S) to (T), which is the solution to problem (10).

From Eq. (11) follows that,

$$g_{k+1}^*(x_{k+1}) = \min_{x_0, \dots, x_k} \sum_{j=0}^{k+1} g(x_{j-1}, x_j) \quad (12)$$

$$= \min_{x_k} \left\{ \min_{x_0, \dots, x_{k-1}} \left(\sum_{j=0}^k g(x_{j-1}, x_j) + g(x_k, x_{k+1}) \right) \right\} \quad (13)$$

$$= \min_{x_k} \left\{ \min_{x_0, \dots, x_{k-1}} \left(\sum_{j=0}^k g(x_{j-1}, x_j) \right) + g(x_k, x_{k+1}) \right\}, \quad (14)$$

which results in the DP recursion formula,

$$g_{k+1}^*(x_{k+1}) = \min_{x_k} (g_k^*(x_k) + g(x_k, x_{k+1})). \quad (15)$$

Having established the DP recursion formula, the forward DP algorithm can be used to find the optimal state sequence. Note how the $F_{n_0, i}$ and $T_{n_0, i}$ sets are used to establish the connections between the layers of the multilevel trellis. The utilization of these sets constrains the admissible paths to represent a valid QT.

1. Initialization: for all $x_0 \in T_{n_0,0}$ do,

$$g_0^*(x_0) = g(S, x_0), \quad (16)$$

where S represents the starting node, i.e., an auxiliary node representing the convention for starting the DPCM of the DVF. A pointer, $i(x_k)$ is introduced, which is used to keep track of the optimal path,

$$i(x_0) = S. \quad (17)$$

2. Recursion: for $k = 0, \dots, 4^{N-n_0} - 2$ and for all $x_{k+1} \in T_{n_0,k+1}$ do,

$$g_{k+1}^*(x_{k+1}) = \min_{x_k \in F_{n_0,k}} (g_k^*(x_k) + g(x_k, x_{k+1})), \quad (18)$$

$$i(x_{k+1}) = \arg \min_{x_k \in F_{n_0,k}} (g_k^*(x_k) + g(x_k, x_{k+1})), \quad (19)$$

3. Termination:

$$g_{4^{N-n_0}}^*(T) = \min_{x_{4^{N-n_0}-1} \in F_{n_0,4^{N-n_0}-1}} (g_{4^{N-n_0}-1}^*(x_{4^{N-n_0}-1}) + g(x_{4^{N-n_0}-1}, T)), \quad (20)$$

where T is an auxiliary terminal node used to find the minimum of all optimal cost functions at epoch $4^{N-n_0} - 1$, since for our purpose, $g(x_{4^{N-n_0}-1}, T) = 0$. Again the back pointer is calculated

$$i(T) = \arg \min_{x_{4^{N-n_0}-1} \in F_{n_0,4^{N-n_0}-1}} (g_{4^{N-n_0}-1}^*(x_{4^{N-n_0}-1}) + g(x_{4^{N-n_0}-1}, T)). \quad (21)$$

4. Backtracking: the pointer i is used to backtrack the optimal state sequence.

$$k = N_{\mathcal{T}}, \quad (22)$$

$$x_k^* = T, \quad (23)$$

do

$$k \leftarrow k - 1, \quad (24)$$

$$x_k^* = i(x_{k+1}^*), \quad (25)$$

until

$$x_k^* = S. \quad (26)$$

This leads to the optimal state sequence $x_0^*, \dots, x_{N_{\mathcal{T}}-1}^*$.

In Fig. 6, a QT of depth 4 is displayed and the optimal state sequence is indicated which leads to the segmentation shown in Fig. 7. Note that the resulting scanning path is optimal and the segmentation cost along the optimal path adds up to 13 bits, which is the number of bits needed to encode this QT decomposition. The bit stream for this QT decomposition is “1010000011001”. The time complexity of DP is $O_{DP}(4^{N-n_0} * |S_{n_0,i}|^2)$ which is significantly smaller than the lower bound for the exhaustive search $\Omega_E(|S_{n_0,i}|^{4^{N-n_0}})$. Note that we have assumed that all the $S_{l,i}$ sets are of the same cardinality.

5 Lossy VBSMCVC

So far we have considered lossless VBSMCVC. In this section we study the more interesting case of lossy VBSMCVC. Clearly for a lossy VBSMCVC it does not make sense to minimize the frame rate R_k with no additional constraints, since this would lead to a very high frame distortion D_k .

The most common approach to solve the tradeoff between the frame rate and the frame distortion is to minimize the frame distortion D_k subject to a given maximum frame rate R_{max} . This problem can be formulated in the following way,

$$\min_{x_0, \dots, x_{N_{\mathcal{T}}-1}} D_k(x_0, \dots, x_{N_{\mathcal{T}}-1}), \quad \text{subject to: } R_k(x_0, \dots, x_{N_{\mathcal{T}}-1}) \leq R_{max}. \quad (27)$$

This constrained discrete optimization problem is very hard to solve in general. In fact the approach we propose will not necessarily find the optimal solution but only the solutions which belong to the convex hull of the rate-distortion curve. On the other hand, as we show in Sec. 7, such solutions tend to be quite dense and hence the convex hull approximation is very good.

We solve this problem using the concept of Lagrangian relaxation [18, 21, 22], which is a well known tool in Operations Research. In this application we will use Lagrangian relaxation to relax the constraint so that the relaxed problem can be solved by DP.

First we introduce the Lagrangian cost function which is of the following form,

$$J_{\lambda}(x_0, \dots, x_{N_{\mathcal{T}}-1}) = D_k(x_0, \dots, x_{N_{\mathcal{T}}-1}) + \lambda * R_k(x_0, \dots, x_{N_{\mathcal{T}}-1}), \quad (28)$$

where $\lambda \geq 0$ is called the Lagrangian multiplier. It has been shown in [18, 21, 22] that if there is a λ^* such that,

$$[x_0^*, \dots, x_{N_{\mathcal{T}}-1}^*] = \arg \min_{x_0, \dots, x_{N_{\mathcal{T}}-1}} J_{\lambda^*}(x_0, \dots, x_{N_{\mathcal{T}}-1}), \quad (29)$$

and which leads to $R_k(x_0^*, \dots, x_{N_{\mathcal{T}}-1}^*) = R_{max}$, then $x_0^*, \dots, x_{N_{\mathcal{T}}-1}^*$ is also an optimal solution to (27). It is well known that when λ sweeps from zero to infinity, the solution to problem (29) traces out the convex

hull of the rate distortion curve, which is a non-increasing function. Hence bisection [23] or the fast convex search we presented in [17] can be used to find λ^* .

Therefore the problem at hand is to find the optimal solution to the problem expressed in Eq. (29). We will show how the original DP approach can be modified to find the global minimum of the problem expressed in Eq. (29). For a given λ , let the $g(x_{j-1}, x_j)$ function be defined as follows,

$$g(x_{j-1}, x_j) = d(x_j) + \lambda * r(x_{j-1}, x_j), \quad (30)$$

where as in the lossless VBSMCVC case, $r(x_{j-1}, x_j)$ equals $R^{SEG}(x_j) + R^{QDFD}(x_j) + R^{DVF}(x_{j-1}, x_j)$. This implies that, $G(x_0, \dots, x_{N_{\mathcal{T}}-1}) = J_{\lambda}(x_0, \dots, x_{N_{\mathcal{T}}-1})$. Hence the DP algorithm presented in section 4 leads to the optimal solution of the problem expressed in Eq. (29).

Note that the dual problem, which can be stated as follows,

$$\min_{x_0, \dots, x_{N_{\mathcal{T}}-1}} R_k(x_0, \dots, x_{N_{\mathcal{T}}-1}), \quad \text{subject to: } D_k(x_0, \dots, x_{N_{\mathcal{T}}-1}) \leq D_{max}. \quad (31)$$

can be solved with exactly the same technique using the following relabeling of function names,

$$R_k(x_0, \dots, x_{N_{\mathcal{T}}-1}) \leftarrow D_k(x_0, \dots, x_{N_{\mathcal{T}}-1}) \text{ and } D_k(x_0, \dots, x_{N_{\mathcal{T}}-1}) \leftarrow R_k(x_0, \dots, x_{N_{\mathcal{T}}-1}).$$

6 Implementation

So far the general theory for a VBSMCVC has been discussed. In this section, as an example of the above theory, a video coder is presented which is based on the introduced theory. This coder is henceforth called the optimal DCT-QT-coder, or for short the optimal coder. In this scheme, the lossy encoding of the DFD is accomplished in the DCT domain, which is the most common way of encoding the DFD. In fact the DCT, quantization, run length and entropy coding are exactly the same as in TMN4 [24].

In TMN4, the quantizer step size QP can have 31 different values but for the presented results QP was fixed to be equal to 10. The only exception to this is the “constant distortion” scheme presented later on, where QP is set to 11. In the presented implementation, each block has an encoding mode which can be Skip, Prediction, Inter or Intra. If the encoding mode is set to Skip, then the block is just replaced by the block at the same location in the previously reconstructed frame. In the case of the Prediction encoding mode, the block is replaced by a motion compensated block from the previously reconstructed frame but still, no DFD is sent. The Inter mode differs from the Prediction mode in that the lossy encoded DFD is sent also. If the Intra mode is selected, then no prediction is used and the block is just Intra encoded, i.e., the original image block is encoded. The quantizer step size $QP = 10$ and the encoding modes of a given block lead to the set of all admissible quantizers, $Q_{l,i} = \{\text{Skip, Prediction, Inter, Intra}\} \times \{10\}$.

The rate distortion points of the Intra and Inter nodes at level $n_0 = 3$ are calculated in the DCT domain. For bigger block sizes, the rate distortion points are calculated by using the rate distortion points of their child nodes. This can be achieved since in the presented implementation, blocks greater than 8×8 which are Inter or Intra coded are encoded by coding their 8×8 child nodes.

In the presented examples, the optimal coder works with video sequences which are in the quarter common intermediate format (QCIF), which is of dimensions 176×144 pixels. The theory has been developed for images of the size $2^n \times 2^n$ where n is an integer, but it can be easily adapted to another image format such as QCIF.

The smallest block size in the employed QT decomposition is 8×8 ($n_0 = 3$) and the largest block size is 256×256 ($N = 8$). Since the QCIF format is 176×144 , the 256×256 QT has been pruned such that only nodes which correspond to an image region are considered. Hence some of the nodes have fewer than four children and this is taken into account when the segmentation cost is distributed recursively. The smallest block size is set to 8×8 since the efficiency of the run length coding drops significantly for 4×4 blocks. Clearly a vector quantization based scheme could easily include 4×4 blocks or even smaller ones but for this implementation, only a DCT based encoding of the DFD has been considered which will lead to a fair comparison in Section 7, since the comparison coder and the optimal coder work with the same DFD encoding technology.

The optimal scanning path has been developed for an image of size $2^n \times 2^n$ where n is an integer. Since the proposed coder is applied to QCIF sequences (176×144) only the 128×128 block in the lower left corner is scanned by a pure Hilbert scan and the rest of the image is scanned in a Hilbert-like fashion. The modified Hilbert scan for the 8×8 blocks at level $n_0 = 3$ used for the QCIF video sequences is displayed in Fig. 8. Note this scan is still optimal since the condition used in the proof of lemma 1 also holds for this scanning path.

It is well known that the DC values of the luminance (Y) and the chrominance channels (Cb, Cr) of neighboring blocks are highly correlated and therefore an encoding scheme should take advantage of this. One way of exploiting this fact is by encoding the DC values of consecutive intra blocks by first order DPCM. Therefore an additional dependency has been introduced and $r(x_{j-1}, x_j)$ of Eq. (30) is now equal to

$$r(x_{j-1}, x_j) = R^{SEG}(x_j) + R^{QDFD}(x_j) + R^{DVF}(x_{j-1}, x_j) + R^{DC}(x_{j-1}, x_j), \quad (32)$$

where $R^{DC}(x_{j-1}, x_j)$ is zero whenever the blocks associated with x_{j-1} and x_j are not both Intra coded, and equal to the number of bits needed to encode the difference between the DC coefficients of the two

Intra coded blocks, otherwise. The DPCM of the DC values is extremely important for an Intra frame. Hence by using this DPCM the proposed coder will also efficiently encode an Intra frame, such as the first frame of a sequence.

From a theoretical point of view, every possible motion vector of block $b_{l,i}$ should be included in the set $M_{l,i}$. This means that for a typical search window of ± 15 pixels and an accuracy of $1/2$ pixel, $|M_{l,i}| = 63 * 63 = 3969$, which is quite large. Most of these motion vectors, however, are not likely candidates for the optimal path, since they do not correspond well to the real motion in the scene and therefore they lead to a high distortion and a high rate.

To make the optimization process faster, such prior knowledge should be taken into account. Even though this is complicated in general, it can be easily achieved in the presented framework of dynamic programming by reducing the set $M_{l,i}$ of admissible motion vectors of block $b_{l,i}$. In the presented implementation, an initial motion vector search is first conducted for the 8×8 blocks at level $n_0 = 3$ by doing a block matching with integer accuracy. The K integer motion vectors which lead to the best prediction are kept, where $K = 10$ for the presented implementation. Then the set $M_{n_0,i}$ is defined as the set which contains the K top integer motion vectors plus their half pixel neighbors. Since the Skip and Intra encoding mode imply a zero motion vector the resulting set of all admissible state values of block $b_{n_0,i}$, $S_{n_0,i}$, is defined as follows,

$$S_{n_0,i} = \{n_0\} \times \{i\} \times \{10\} \times \left((\{\text{Skip, Intra}\} \times \{\vec{0}\}) \cup (\{\text{Prediction, Inter}\} \times M_{n_0,i}) \right). \quad (33)$$

After the set of the admissible state values has been defined for the bottom layer (n_0), the sets of the admissible state values for higher level blocks can be defined recursively in a Bottom-Up fashion, by calling the function “states(l, i)” below with the following parameters: states($N, 0$).

states(l, i)

if ($l = n_0 + 1$)

$$S_{l,i} = \{l\} \times \{i\} \times \{10\} \times \left((\{\text{Skip, Intra}\} \times \{\vec{0}\}) \cup (\{\text{Prediction, Inter}\} \times (\bigcap_{j=0}^3 M_{l-1, 4*i+j})) \right);$$

else

$$\text{states}(l - 1, 4 * i + 0); \text{states}(l - 1, 4 * i + 1); \text{states}(l - 1, 4 * i + 2); \text{states}(l - 1, 4 * i + 3);$$

$$S_{l,i} = \{l\} \times \{i\} \times \{10\} \times \left((\{\text{Skip, Intra}\} \times \{\vec{0}\}) \cup (\{\text{Prediction, Inter}\} \times (\bigcap_{j=0}^3 M_{l-1, 4*i+j})) \right);$$

In other words, a block $b_{l,i}$ only includes a motion vector in $S_{l,i}$ if the motion vector has been selected by all of its child nodes. This leads to the fact that for small blocks, many motion vectors are considered but the bigger the blocks get, the fewer motion vectors are included. This reflects the well known fact that

small block sizes lead to small energy in the DFD but not very consistent motion vector fields, whereas bigger blocks lead to consistent vector fields, but the energy in the DFD can be quite high [8].

Our experiments have shown that for $K = 10$ this restriction of the search space does not lead to a performance loss but increases the speed of the algorithm significantly.

7 Experimental Results

In this section, the results of the proposed coder are compared to test model 6 (TMN6) from TELENOR of the H.263 [7] standard. Note that the optimal coder, like TMN6, writes a bit stream which is uniquely decodable by our decoder. Hence the listed bit rates are the effective number of bits used and not an estimate of the entropy.

TMN6 is selected as the comparison coder since it is a very low bit rate coder. At very low bit rates, the side information, such as motion vectors and encoding modes, take up a bigger percentage of the overall bit rate than for a higher bit rate coder and therefore the performance difference between the optimal coder and a coder which uses a fixed block size and an encoding heuristics should be more pronounced. Also the optimal coder uses a very similar block based DCT encoding of the DFD (from TMN4) as TMN6 and it has the same range for the motion estimation which leads to a fair comparison between the two coders. TMN6 has two advantages over the optimal coder implementation, which uses parts of TMN4. First, the variable length code for the DCT coefficients is more efficient and second, the prediction is based on overlapped block motion compensation. Nevertheless, we use TMN6 with the “Advanced Prediction Mode” switched on for comparison purposes, and not TMN4, since it is currently one of the best very low bit rate video coder.

In order to compare TMN6 and the optimal coder, TMN6 was used to encode every 4th of the first 200 frames of the QCIF sequence “Mother and Daughter” with a fixed quantizer step size $QP = 10$. The first frame was Intra coded with the above quantizer step size, for both TMN6 and the optimal coder. Since the “Mother and Daughter” sequence is considered to be recorded at 30 frames/second, this leads to an encoded frame rate of 7.5 frames/second. The optimal coder implementation encodes only the luminance component (Y) of the sequence. Hence we set the chrominance part of the sequence to zero and subtracted the bits used to encode the DCT color coefficients from the resulting TMN6 rates. The resulting rate and distortion were used for the comparison between TMN6 and the optimal coder. The employed distortion measure is the peak signal to noise ratio (PSNR) which is defined as the peak signal power of an 8 bit sequence (255^2) divided by the mean squared error (MSE), that is, $PSNR = 10 * \log_{10} (255^2 / MSE)$.

7.1 Matched distortion

The goal of this experiment is to compare the optimal coder with TMN6 in the case where their frame distortions are matched. This can be achieved by setting D_{max} , the maximum frame distortion from Eq. (31) equal to the frame distortion of TMN6. Clearly D_{max} changes from frame to frame, following the distortion profile of the TMN6 run. The optimal coder will lead to the smallest number of bits needed to encode a given frame for the given maximum distortion D_{max} .

The resulting rate and distortion are displayed in Fig. 9. The average rate and distortion for the entire sequence are listed in Table 1. The distortion of the proposed coder follows the TMN6 distortion extremely closely. Clearly the proposed coder is superior to TMN6 when their frame distortions are matched, based on the resulting difference (2.6 kbits/s on the average) in bit rates.

The optimal QT segmentation, the optimal encoding mode selection and the optimal motion vector field are displayed in Fig. 10 for the 16th frame of the “Mother and Daughter” sequence. It is evident in Fig. 10 that the smaller block sizes are used at object boundaries where the motion vector field is discontinuous and the larger blocks are used in background areas which are stationary. Note in Fig. 10 how the new object (hand) and the uncovered areas (left of the hand) are intra coded and the stationary background is replaced by the blocks from frame 12 (Skip mode). As can be seen in Fig. 10, the Skip and the Prediction modes are the most commonly used encoding modes. In fact, for the entire sequence, without the first image, the Skip mode is used for 57.4% of the image, the Prediction mode is used for 27.0% of the image, the Inter mode is used for 14.1% of the image and the Intra mode is used for 1.5% of the image. In other words, the DFD is only sent for 15.6% of the image whereas for 84.4% of the image no DFD is sent. This is achieved by the superior motion compensation of this variable block size approach.

7.2 Matched rate

In this experiment, the proposed coder is compared to TMN6 in the case where their frame rates are matched. This can be achieved by setting R_{max} , the maximum frame rate from Eq. (27) equal to the frame rate of TMN6. Clearly R_{max} changes from frame to frame, following the rate profile of TMN6 and the proposed coder will minimize the resulting frame distortion for the given frame rate.

The resulting rate and distortion are displayed in Fig. 11. The average rate and distortion for the entire sequence are shown in Table 1. Again, note that the rate of the proposed coder follows the TMN6 rate very closely. Besides being able to outperform TMN6 for matched rates, this experiment also shows the enormous potential of this approach with respect to rate control since the optimal coder can follow an

arbitrary bit assignment per frame and produce the smallest possible distortion for the given bit budget. Furthermore the resulting sequence is clearly of a higher visual quality than the TMN6 sequence, since a better motion compensation is accomplished and more bits are available to encode the DFD.

7.3 Constant distortion

So far TMN6 and the proposed coder have been compared in terms dictated by the TMN6 run. This gives TMN6 an advantage, since it can set the rate distortion profile which then has to be followed by the proposed coder.

An interesting application of the proposed coder is for channels which can accept a variable bit rate, such as an ATM network. For such applications, one would like to keep the distortion constant which can be achieved by setting D_{max} , the maximum frame distortion from Eq. (31), equal to the desired frame distortion. The proposed coder allows therefore for the encoding of a video sequence with constant frame quality.

For the experiment discussed next, D_{max} was selected to be equal to the minimum frame PSNR of the TMN6 run, since this is the best quality TMN6 can guarantee over the entire sequence. In this experiment, the distortion is constant for each frame of the sequence, and hence the average distortion is equal to the frame distortion, which is equal to the maximum frame distortion of TMN6. Therefore the fixed quantizer step size QP , which is equal to 10 in the TMN6 run, is set to 11 for the constant distortion experiment, since a coarser quantizer step size is required for a higher average distortion. For the first frame the quantizer is automatically selected so that its distortion is as close as possible to the desired constant frame distortion. The resulting rate and distortion are displayed in Fig. 12. The average rate and distortion for the entire sequence are in Table 1. Clearly the goal of constant distortion (quality) has been achieved and the resulting average rate is much lower than the TMN6 rate, even though visually these two encoded sequences cannot be distinguished. Some observers even prefer the constant quality sequence over the TMN6 sequence. One possible explanation for this fact is based on the globally optimal selection of the DFD and the DVF. Recall that a Hilbert scan is used for the DPCM encoding of the DVF and a smooth DVF along this path leads to a low bit rate. Hence the optimal solution enforces a global smoothness constraint on the DVF which in turn leads to predicted frames which are more visually pleasing than the ones block matching produces.

So far all the experiments presented have been based on the “Mother and Daughter” sequence. In the field of very low bit rate video coding, a common test sequence is the “Miss America” sequence. It is well known that the motion in this sequence is almost completely translational and therefore this sequence

should be well modeled by the proposed variable block size encoder. Again, the “Miss America” sequence is a QCIF sequence of which every 4th luminance (Y) frame is encoded which leads to an encoded frame rate of 7.5 frames per second. The sequence is coded with a quantizer step size of 12 and the target distortion is 35.0 dB PSNR. The resulting average bit rate is 5.7 kbits per second and the average distortion is 35.0 dB PSNR.

This extremely low bit rate for this high PSNR value can be explained by looking at the encoding modes. The prediction of the future frames is so successful that the DFD has to be sent for less than 6% of the sequence. In other words, the Intra or Inter modes are only used to update the scene for less than 6% of the total image size. These 6% can be considered model failure regions and then they can be directly compared to the 4% model failure regions in the object oriented approach presented in [9]. As expected, the Intra and Inter modes are most often used around the eyes and the mouth.

8 Summary and conclusions

We have proposed an optimal scanning path for a quad-tree (QT) decomposition which is based on a Hilbert curve. For this purpose, we have introduced a QT based recursive generation of a Hilbert curve. We have presented a general theory for the optimal bit allocation among QT segmentation, displacement vector field (DVF) and displaced frame difference (DFD). The theory can be applied to all variable block size motion compensated video coders (VBSMCVC), where the variable block sizes are encoded using a QT structure, the DVF is encoded by first order DPCM, the DFD is encoded by a block based scheme and an additive distortion measure is employed.

We first considered a lossless VBSMCVC and derived the optimal bit allocation algorithm which is based on dynamic programming (DP). We then addressed the problem of lossy VBSMCVC and we showed that Lagrangian relaxation and DP can find the convex hull approximation to the optimal solution. By separating the lossless and the lossy case we were able to show the independence between the Lagrangian multiplier method and the DP approach. These two are usually present as one algorithm even though any scheme which finds an optimal solution to the lossless case can be used in the Lagrangian multiplier approach.

As an example of the proposed theory, a DCT based implementation of an optimal coder has then been discussed and the results of this coder have been presented. We showed that this DCT-QT coder can outperform TMN6 in the rate-distortion sense.

Besides being able to outperform TMN6, the proposed coder is well suited for a rate control scheme,

since for any given bit rate, it will encode the current frame with the smallest possible distortion. Also, the optimal solution enforces a global smoothness constraint on the DVF which in turn leads to predicted frames which are more visually pleasing than the ones produced by block matching. Hence the encoded sequences are not only superior in a rate distortion sense but also in the subjective sense.

We advocate that the theory developed in this paper is used to create efficient video coders which fit into the proposed framework. This will assure an optimal bit allocation among segmentation, motion and residual error and hence no heuristics are necessary to find the encoding parameters. As the experiments have shown, developing a video coder with its optimization in mind can result in a very powerful overall scheme.

References

- [1] R. Forchheimer and T. Kronander, “Image coding—from waveforms to animation,” *Proceedings of the International Conference on Acoustics, Speech and Signal Processing*, vol. 37, pp. 2008–2023, Dec. 1989.
- [2] H. G. Musmann, P. Pirsch, and H. Grallert, “Advances in picture coding,” *Proceedings of the IEEE*, vol. 73, pp. 523–548, Apr. 1985.
- [3] A. K. Jain, “Image data compression: A review,” *Proceedings of the IEEE*, vol. 69, pp. 349–389, Mar. 1981.
- [4] “Coding of moving pictures and associated audio for digital storage media at up to about 1.5 mbits/s.” International Standard ISO/IEC IS-11172, Oct. 1992.
- [5] “Generic coding of moving pictures and associated audio.” International Standard ISO/IEC IS-13818, Nov. 1994.
- [6] ITU-T Recommendations H.261, *Video codec for audiovisual services at $p \times 64$ kbits,*.
- [7] Expert’s group on very low bit rate video telephony, ITU-Telecommunication standardization sector, *Draft Recommendation H.263*.
- [8] M. Bierling, “Displacement estimation by hierarchical blockmatching,” in *Proceedings of the Conference on Visual Communications and Image Processing*, vol. 1001, pp. 942–951, SPIE, 1988.
- [9] M. Hötter, “Object-oriented analysis-synthesis coding based on moving two-dimensional objects,” *Signal Processing: Image Communication*, vol. 2, pp. 409–428, Dec. 1990.
- [10] J. Lee, “Optimal quadtree for variable block size motion estimation,” in *Proceedings of the International Conference on Image Processing*, vol. 3, pp. 480–483, Oct. 1995.
- [11] G. J. Sullivan and R. L. Baker, “Efficient quadtree coding of images and video,” *IEEE Transactions on Image Processing*, vol. 3, pp. 327–331, May 1994.
- [12] P. Strobach, “Tree-structured scene adaptive coder,” *IEEE Transactions on Communications*, vol. 38, Apr. 1990.

- [13] F. Moscheni, F. Dufaux, and H. Nicolas, "Entropy criterion for optimal bit allocation between motion and prediction error information," in *Proceedings of the Conference on Visual Communications and Image Processing*, vol. 2094, pp. 235–242, SPIE, 1993.
- [14] J. Ribas-Corbera and D. L. Neuhoff, "Optimal bit allocations for lossless video coders: motion vectors vs. difference frames," in *Proceedings of the International Conference on Image Processing*, vol. 2, pp. 180–183, 1995.
- [15] T. Wiegand, M. Lightstone, T. G. Campbell, and S. K. Mitra, "Efficient mode selection for block based motion compensated video coding," in *Proceedings of the International Conference on Image Processing*, vol. 2, pp. 559–562, Oct. 1995.
- [16] T. Wiegand, M. Lightstone, D. Mukherjee, T. G. Campbell, and S. K. Mitra, "Rate-distortion optimized mode selection for very low bit rate video coding and the emerging H.263 standard," *Transactions on Circuits and Systems for Video Technology*, vol. 6, pp. 182–190, Apr. 1996.
- [17] G. M. Schuster and A. K. Katsaggelos, "Fast and efficient mode and quantizer selection in the rate distortion sense for H.263," in *Proceedings of the Conference on Visual Communications and Image Processing*, pp. 784–795, SPIE, Mar. 1996.
- [18] K. Ramchandran, A. Ortega, and M. Vetterli, "Bit allocation for dependent quantization with applications to multiresolution and MPEG video coders," *IEEE Transactions on Image Processing*, vol. 3, pp. 533–545, Sept. 1994.
- [19] G. M. Schuster and A. K. Katsaggelos, "A video compression scheme with optimal bit allocation between displacement vector field and displaced frame difference," in *Proceedings of the International Conference on Acoustics, Speech and Signal Processing*, May 1996.
- [20] D. P. Bertsekas, *Dynamic programming: Deterministic and stochastic models*. Prentice-Hall, 1987.
- [21] Y. Shoham and A. Gersho, "Efficient bit allocation for an arbitrary set of quantizers," *IEEE Transactions on Acoustics, Speech and Signal Processing*, vol. 36, pp. 1445–1453, Sept. 1988.
- [22] H. Everett, "Generalized Lagrange multiplier method for solving problems of optimum allocation of resources," *Operations Research*, vol. 11, pp. 399–417, 1963.
- [23] C. F. Gerald and P. O. Wheatley, *Applied numerical analysis*. Addison Wesley, fourth ed., 1990.

- [24] Expert's Group on Very Low Bitrate Visual Telephony, *Video Codec Test Model, TMN4 Rev1*. ITU Telecommunication Standardization Sector, Oct. 1994.
- [25] G. M. Schuster and A. K. Katsaggelos, *Rate-distortion based video compression, Optimal video frame compression and object boundary encoding*. Kluwer academic publishers, 1997.

BIOGRAPHICAL SKETCH

Guido M. Schuster received the Ing HTL degree in Elektronik, Mess- und Regeltechnik in 1990 from the Neu Technikum Buchs (NTB), Buchs, St.Gallen, Switzerland. At the NTB, he was awarded the gold medal for academic excellence, and was also the winner of the first annual Landis & Gyr fellowship competition.

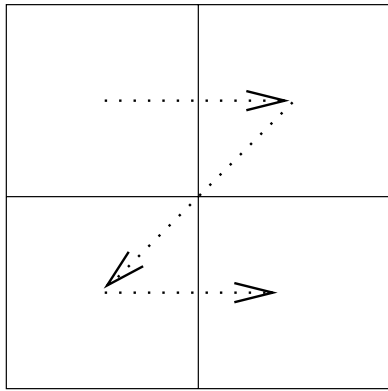
Dr. Schuster received the M.S. and Ph.D. degrees, both in Electrical Engineering, from Northwestern University, Evanston, Illinois, in 1992 and 1996, respectively. In 1996 he joined the Network Systems Division of U.S. Robotics in Mount Prospect, Illinois, where he co-founded the Advanced Technologies Research Center and where he is currently the Head of Future Technologies.

Dr. Schuster has filed and holds several patents in fields ranging from adaptive control over video compression to Internet telephony. He also is the co-author of the book "Rate-Distortion based Video Compression", published by Kluwer Academic Publishers. His current research interests are Telepresence, Operational Rate-Distortion Theory and Networked Multimedia.

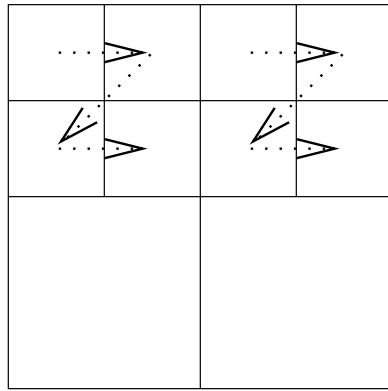
Aggelos K. Katsaggelos received the Diploma degree in electrical and mechanical engineering from the Aristotelian University of Thessaloniki, Thessaloniki, Greece, in 1979 and the M.S. and Ph.D. degrees both in electrical engineering from the Georgia Institute of Technology, Atlanta, Georgia, in 1981 and 1985, respectively.

In 1985 he joined the Department of Electrical Engineering and Computer Science at Northwestern University, Evanston, IL, where he is currently professor. During the 1986-1987 academic year he was an assistant professor at Polytechnic University, Department of Electrical Engineering and Computer Science, Brooklyn, NY. His current research interests include image recovery, processing of moving images (motion estimation, enhancement, very low bit rate compression), computational vision, and multimedia signal processing. Dr. Katsaggelos is an Ameritech Fellow and a member of the Associate Staff, Department of Medicine, at Evanston Hospital. He is a senior member of IEEE, and also a member of SPIE, the Steering Committees of the *IEEE Transactions on Medical Imaging* and the *IEEE Transactions on Image Processing*, the IEEE Technical Committees on Visual Signal Processing and Communications, Image and Multi-Dimensional Signal Processing, and Multimedia Signal Processing, the Technical Chamber of Commerce of Greece and Sigma Xi. He has served as an Associate editor for the *IEEE Transactions on Signal Processing* (1990-1992), an area editor for the journal *Graphical Models and Image Processing* (1992-1995), and he is currently the editor-in-chief of the *IEEE Signal Processing Magazine*. He is the editor of *Digital Image Restoration* (Springer-Verlag, Heidelberg, 1991), and co-author of *Rate-Distortion*

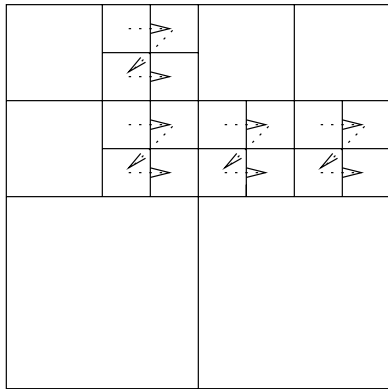
Based Video Compression (Kluwer Academic Publishers, 1997). He has served as the General Chairman of the 1994 Visual Communications and Image Processing Conference (Chicago, IL), and he will serve as the technical program co-chair of the 1998 IEEE International Conference on Image Processing (Chicago, IL).



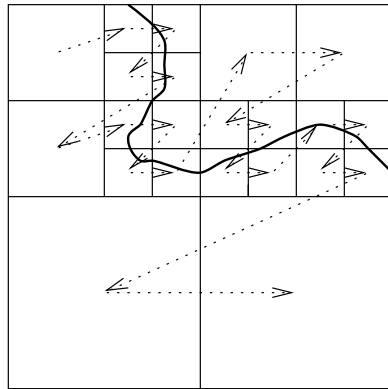
(a)



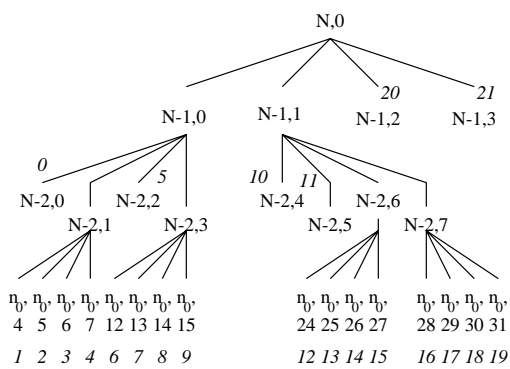
(b)



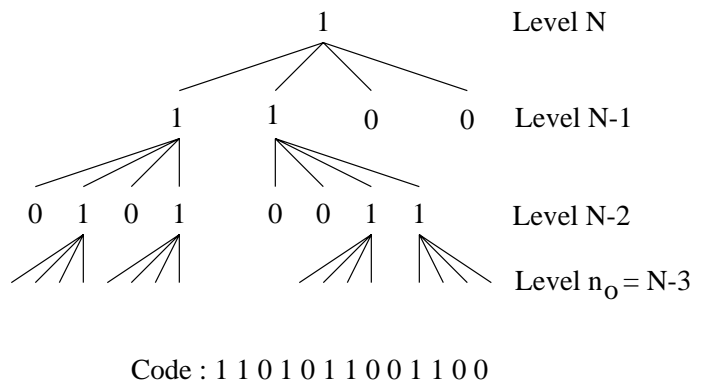
(c)



(d)



(e)



(f)

Figure 1: Quad-tree structure: (a)-(c) scanning path of the different levels; (d) Image block with data to be represented and overall scanning path; (e) node indices and leaf ordering; (f) encoded quad-tree

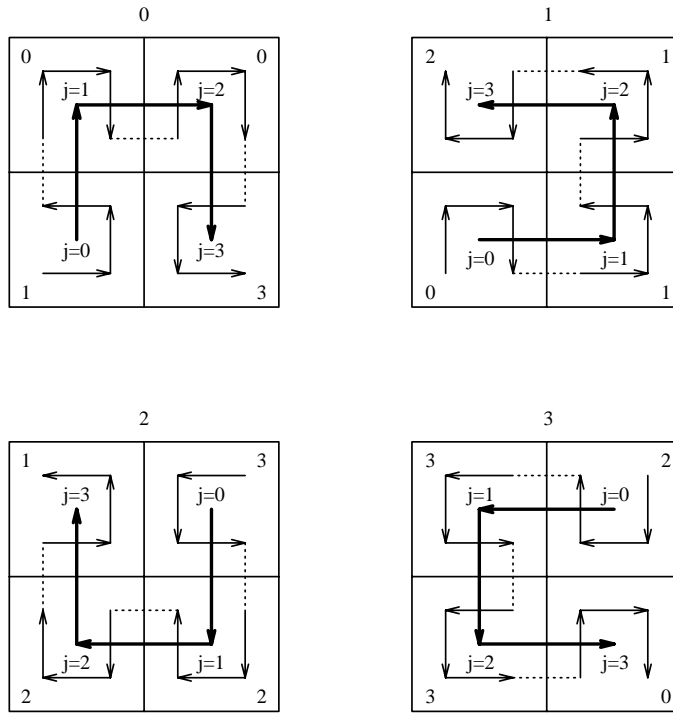


Figure 2: The four possible first order Hilbert curves (-) with the respective second order Hilbert curves underneath (-). The orientations $O_{l,i}$ are shown on top of the squares and the orientations $O_{l-1,4*i+j}$ are shown in the corners of the smaller squares.

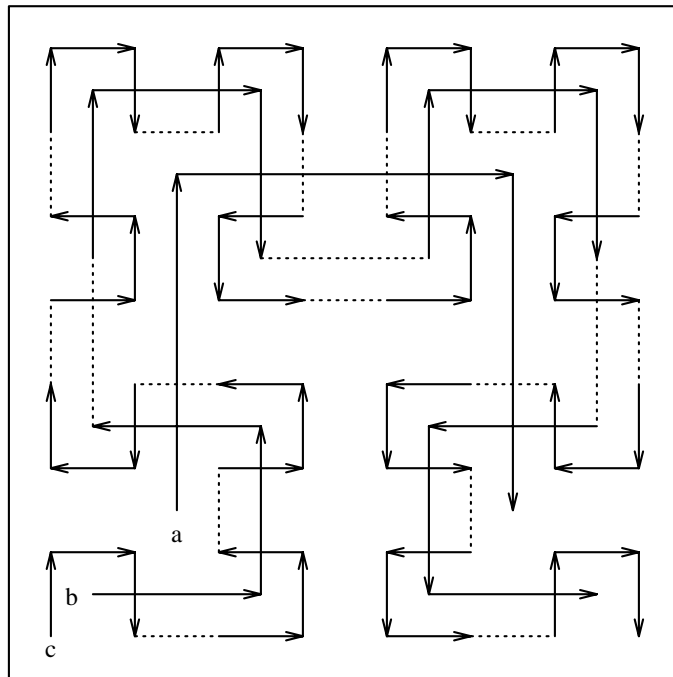


Figure 3: Recursive Hilbert curve generation: a) first order Hilbert curve of orientation 0, b) second order Hilbert curve, c) third order Hilbert curve

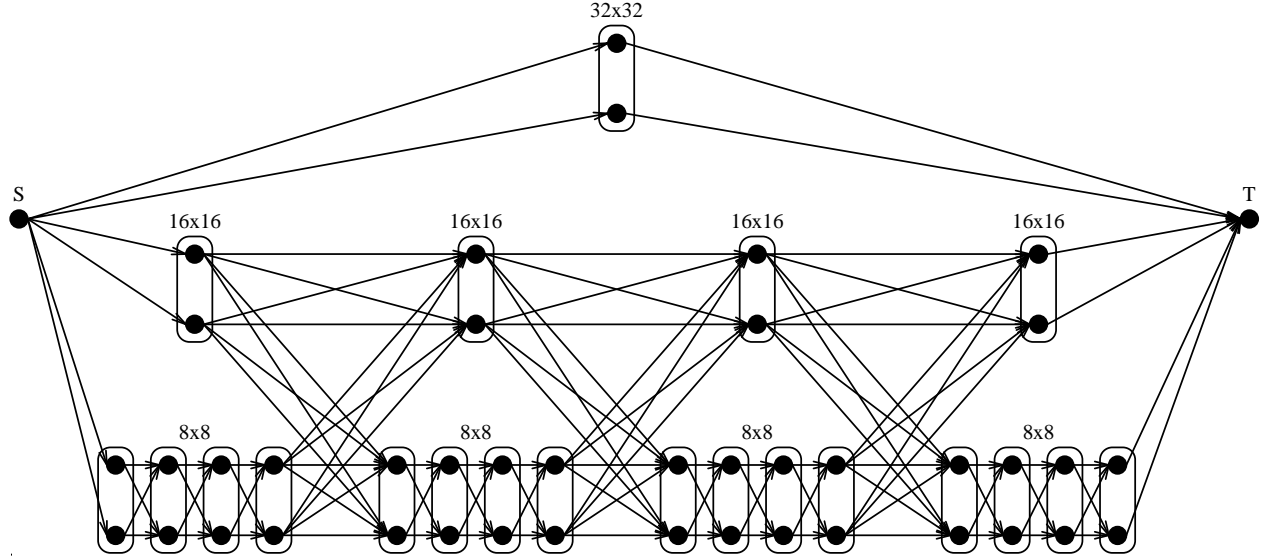


Figure 4: The multilevel trellis for $N = 5$ and $n_0 = 3$

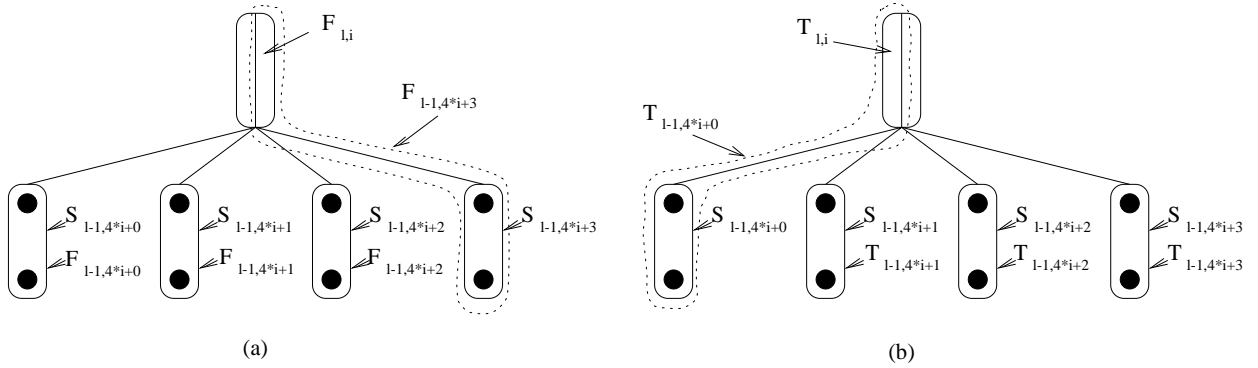


Figure 5: The recursive rule for the generation of the $T_{l,i}$ and $F_{l,i}$ sets

| | average rate kbits/s | average distortion (average PSNR) dB |
|------------------------|-------------------------|---|
| TMN6 | 20.2 | 32.9 |
| matched distortion | 17.6 | 32.9 |
| matched rate | 20.2 | 33.5 |
| constant distortion | 15.5 | 32.3 |

Table 1: Average rate distortion comparison for the “Mother and Daughter” sequence between TMN6 and the proposed optimal coder for different modes of operation

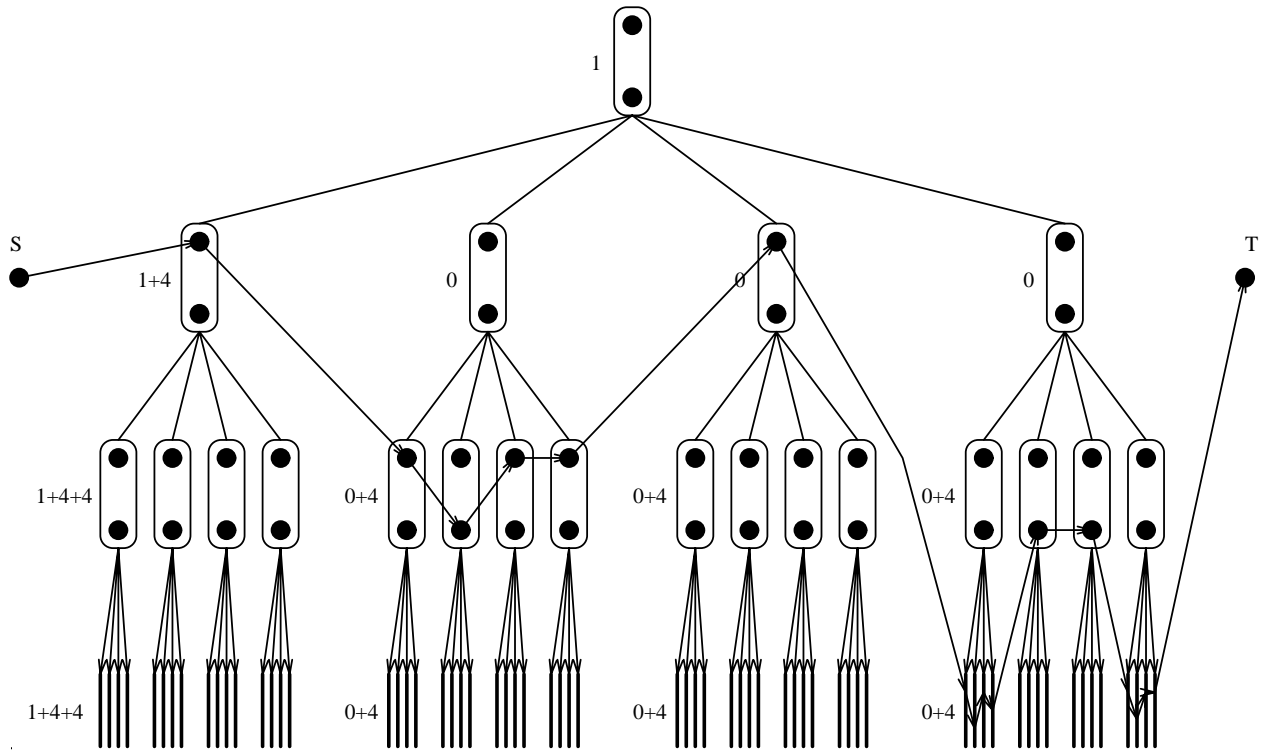


Figure 6: The recursive distribution of the quad-tree encoding cost among the trellis nodes for a quad-tree of depth 4 and the optimal state sequence

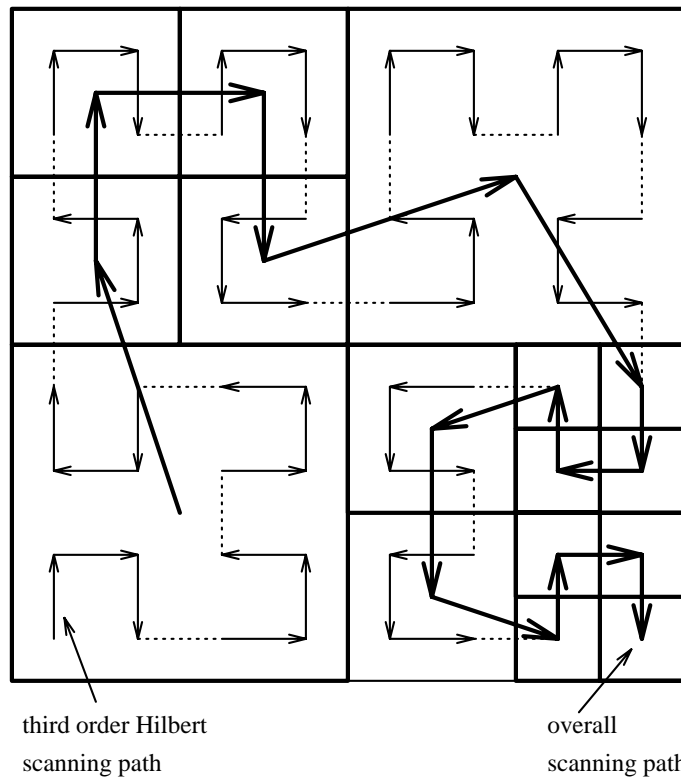


Figure 7: Quad-tree decomposition corresponding to the optimal state sequence

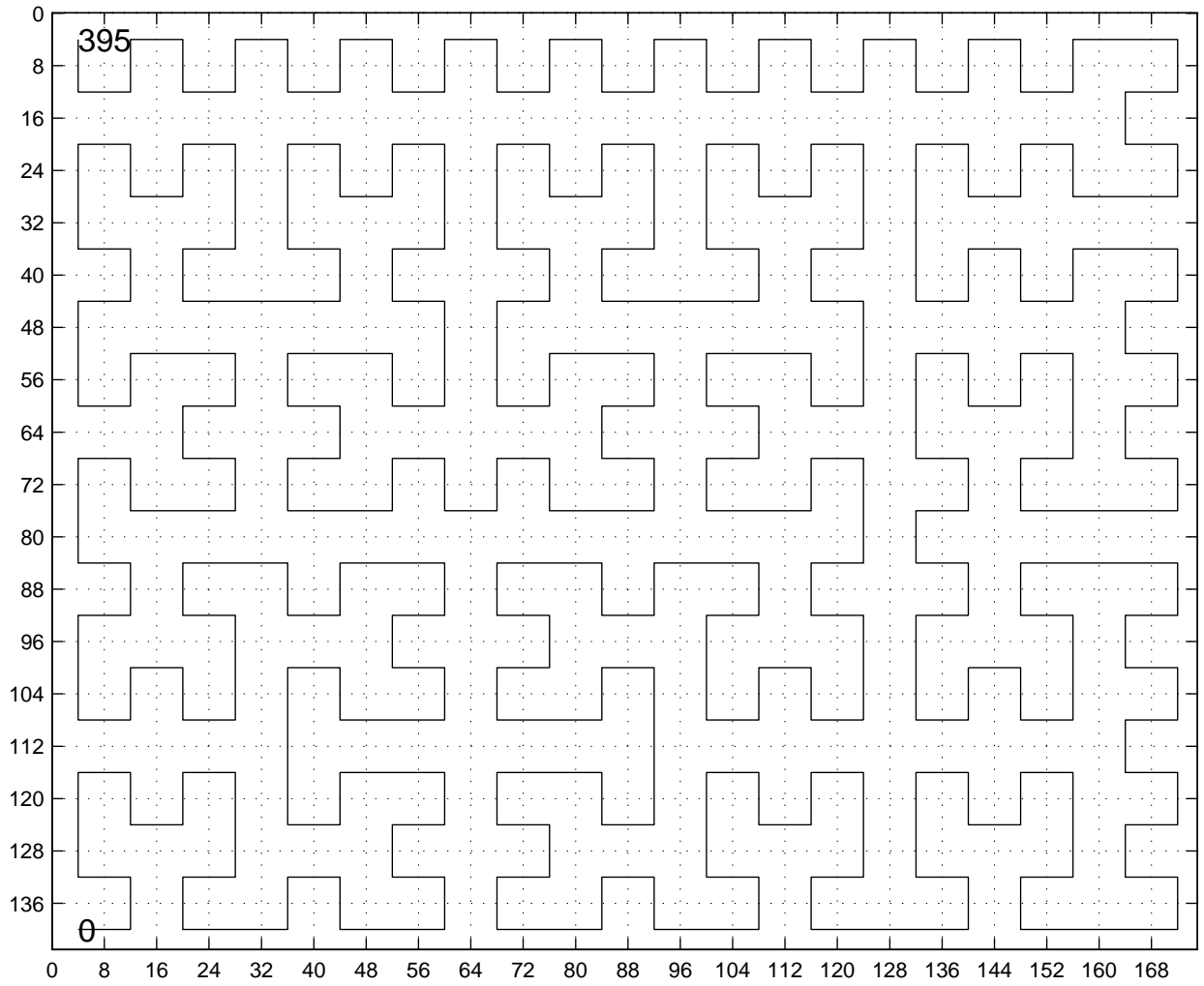


Figure 8: Modified Hilbert scan for level $n_0 = 3$ of a QCIF frame.

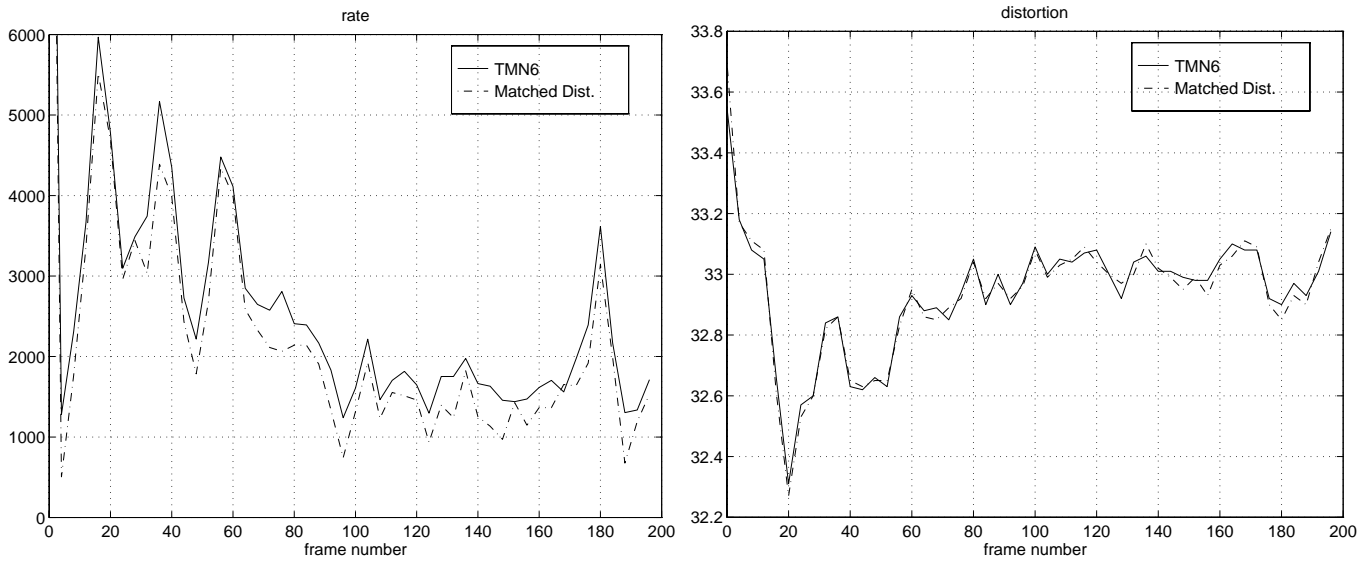


Figure 9: Rate and distortion comparison between TMN6 and the optimal coder, where the TMN6 distortion is the target distortion of the optimal coder.

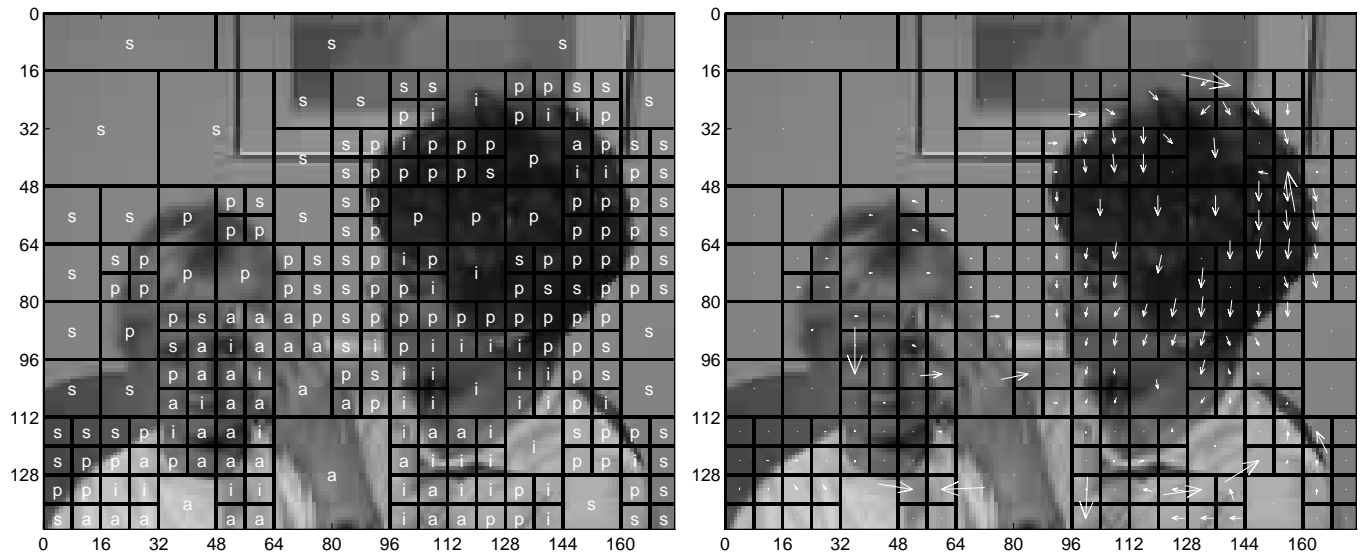


Figure 10: Left: The optimal encoding mode selection, (i) Inter mode, (s) Skip mode, (p) Prediction mode and (a) Intra mode; Right: the optimal DVF, both are for the 16th frame of the “Mother and Daughter” sequence.

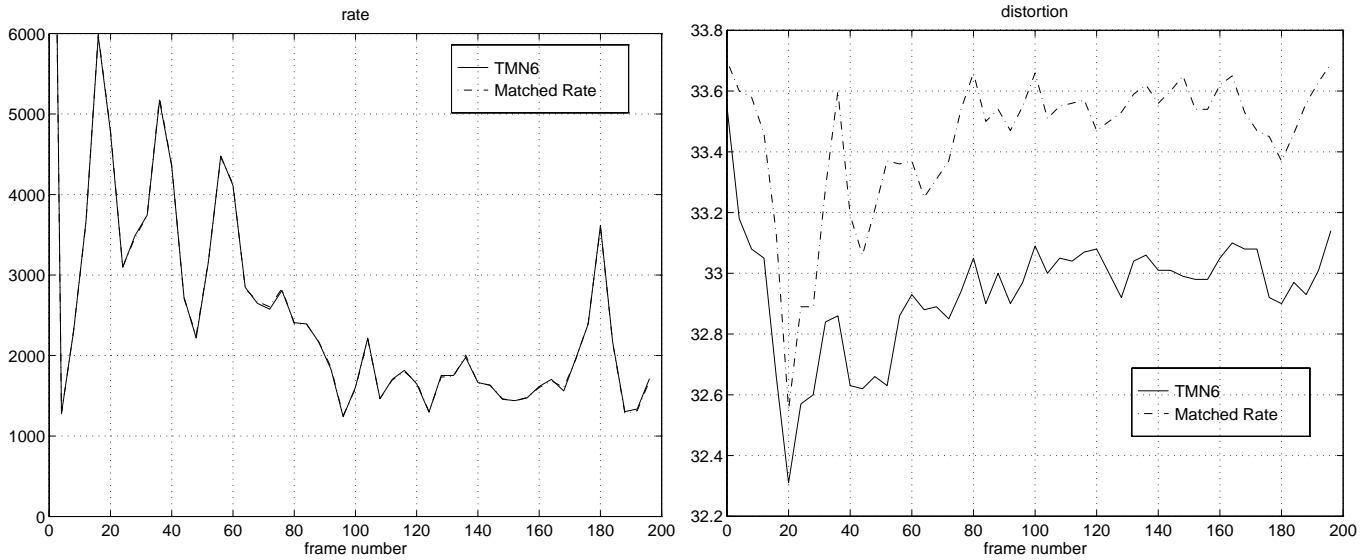


Figure 11: Rate and distortion comparison between TMN6 and the optimal coder, where the TMN6 rate is the target rate of the optimal coder.

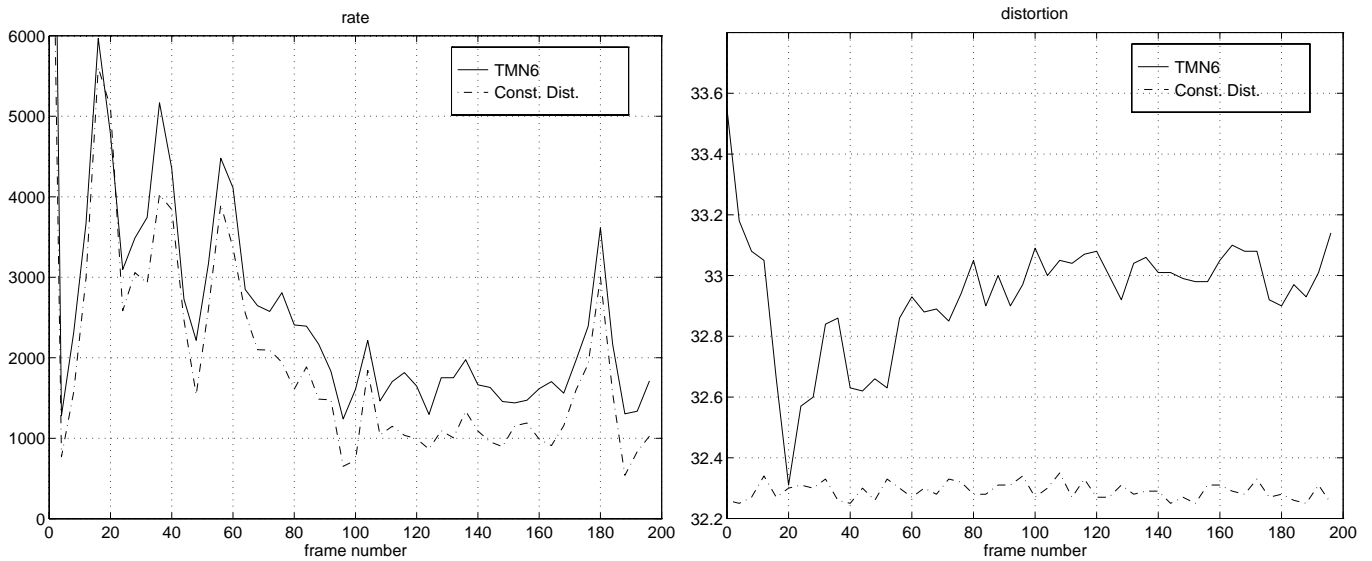


Figure 12: Rate and distortion comparison between TMN6 and the optimal coder, where the distortion of the optimal coder is fixed.